Ethylene–Propylene–Rubber (EPR)/Polydimethylsiloxane (PDMS) Binary Polymer Blends: Morphology and Viscoelastic Properties

M. Carlberg, D. Colombini, F. H. J. Maurer

Department of Polymer Science & Engineering, Lund Institute of Technology, Lund University, Box 124, 22100 Lund, Sweden

Received 13 November 2003; accepted 6 July 2004
DOI 10.1002/app.21171
Published online in Wiley InterScience (www.interscience.wiley.com).

ABSTRACT: Melt mixed blends of ethylene–propylene–rubber (EPR) and polydimethylsiloxane (PDMS) were studied with regard to the composition dependence of the dynamic viscoelastic properties in relation to their morphology. Differential scanning calorimetry, scanning electron microscopy, and dynamic mechanical analysis (DMA) were used together with theoretical predictions to characterize the blends. The investigation of the viscoelastic properties showed significant improvement of the mechanical properties of the blends following the increase of the EPR content. The association of DMA results and theoretical predictions indicated that the studied blends consisted of dispersed PDMS in a matrix of EPR over the whole composition range. The microscopy study of the blends also supports these morphological conclusions. © 2004 Wiley Periodicals, Inc. J Appl Polym Sci 94: 2240–2249, 2004

Key words: polyolefins; polysiloxanes; morphology; viscoelastic properties; blends

INTRODUCTION

Polymer insulators are steadily increasing in their use in high voltage outdoor applications. The main reasons for this are their hydrophobic surfaces and low density compared to ceramic materials. The most commonly used polymeric materials for high voltage insulating applications are ethylene–propylene–diene polymers (EPDM) and polydimethylsiloxane rubbers (PDMS). Both of these materials have good electrical and chemical properties and are resistant to heat and ultraviolet radiation.[1] EPDM as a material has good mechanical properties, whereas the silicones have relatively poor tear and abrasive strengths and are therefore often filled with silicas. The aspect that makes silicone rubbers very interesting is their ability to recover the hydrophobic nature of the surface after damage from corona, discharges, or pollution. This ability is due to the fact that low molecular weight silicone molecules migrate to the surface from the bulk of the material.[2–5] Polymer blends based on silicones and EPDM could combine the properties of these two materials and are therefore of interest.[6–15] Mitchell[6] reported that the combination of the beneficial properties of both EPDM and PDMS was obtained in a composite of these materials, such as tensile strength and moisture resistance. Kole et al.[7–12] have reported in several papers the curing, compatibilization, and hydrothermal weathering of this blend system. The diffusion of small molecules in EPDM/PDMS blends was correlated with the morphology of the blend by Geerts et al.[13]

Polymers are usually thermo dynamically immiscible, which results in heterogeneous blends when they are mixed. Final mechanical properties of a binary system are strongly affected by the state of dispersion of the polymeric inclusions, and smaller particles are usually preferred to achieve good mechanical properties. This can be achieved through compatibilization, where a constituent with chemical and/or physical compatibility with the blend constituents is added to the system. Such a constituent can be either introduced as a premade compatibilizer ("physical compatibilization") or formed *in situ* through reactive compatibilization ("chemical compatibilization").[16] Another way to reach a fine dispersion, without the addition of any new constituent to the system, can be to adjust the intrinsic properties affecting the processing of the blends. Such properties include the molecular weights and the viscosity of the pure constituents, interfacial tension, and shear rate. The viscosity ratio of the pure constituents at the melt mixing temperature is of great importance: it has been shown[17] that the particle size of the dispersed phase can be significantly decreased when the viscosity ratio is close to unity.

Correspondence to: F. H. J. Maurer (frans.maurer@polymer.LTH.se).

TABLE I
Chemical Formulas and Characteristics of the Pure Constituents

Material	Chemical formula	Supplier	Brand name	η_d, at 1 Hz, 180°C	Notes
Ethylene propylene rubber (EPR)	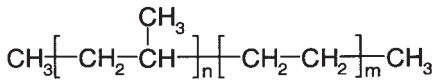	Exxon	Exxelor PE 805	8.95 kPa.s	
Polydimethylsiloxane (PDMS)	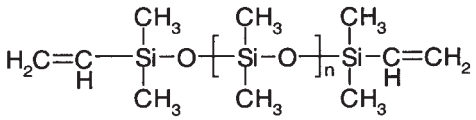	Wacker	Elastosil R401/50	33.33 kPa.s	30 wt % silica

The objective of the present work was to study melt mixed blends of ethylene—propylene–rubber (EPR) and silica-filled PDMS for potential use in high voltage outdoor applications. In particular the dependence of composition on the final mechanical viscoelastic properties of such binary polymer blends is investigated in relation to their morphologies.

EXPERIMENTAL

Materials and sample preparation

The EPR used was Exxelor PE 805 supplied by Exxon Chemical Norden AB, Gothenburg, Sweden. The PDMS used was Elastosil R401/50, a silica-filled polymer from Wacker Chemie GmbH, Burghausen, Germany. The Elastosil contains 30 wt % silica of approximately 100 nm in diameter. Characteristics of the materials are given in Table I.

The binary EPR/PDMS polymer blends were prepared by melt mixing at 180°C for 15 min in a DSM MIDI 2000 corotating twin-screw miniextruder (rotor speed 100 rpm). The samples were then heat pressed at 180°C under 2.2 MPa pressure and cooled in air (at approximately 5°C/min).

Besides the pure constituents, four blend compositions were considered and they are designated 80/20, 60/40, 40/60, and 20/80 according to their EPR/PDMS content in wt %.

Sample characterization

Density measurements were carried out with a Quantachrome Ultrapycnometer 1000 using nitrogen gas. Samples of about 3 g were placed in the measurement cell at a controlled temperature of 26°C. An equilibrium time of 20 min was selected before the measurements, and all density values given in the present article correspond to an average of five measurements with a maximum deviation of 0.05%.

Differential scanning calorimetry (DSC) thermograms were recorded using a Mettler DSC-30 device, under nitrogen atmosphere. The samples were first heated from room temperature to 150°C, to remove the thermal history of the samples. After 5 min isothermal at 150°C, the temperature was then cooled to −145°C at 50°C/min. After a 3-min equilibrium time at −145°C, the samples were heated to 150°C with a heating rate of 10°C/min. The weight of the sample was chosen in the range of 15 ± 2 mg.

A TA Instruments Dynamic Mechanical Analyser, DMA-2980, was used, operating in tensile mode under isochronal conditions at the frequency of 1 Hz to measure the temperature dependence of the dynamic modulus $E_d = |E^*|$and the phase angle δ. The viscoelastic data were recorded from −145 to 130°C with a heating rate of 2°C/min. The samples were approximately 1 mm thick, 5 mm wide, and 13 mm long.

A TA Instruments AR2000 rheometer was used under isothermal conditions at 180°C to measure the frequency dependence of the dynamic viscosity $\eta_d = |\eta^*|$. The rheological measurements were carried out with a frequency sweep from 10^{-3} to 10^2 Hz and a strain of 0.2%. The samples were circular with a diameter of 25 mm and a thickness of approximately 1 mm.

A JEOL JSM-5600LV scanning electron microscope (SEM) was used to analyze the microstructure of the blends. The samples were first cryofractured in liquid nitrogen. To remove the PDMS phase, the samples were then etched in ethyl acetate for 48 h and finally sputtercoated with a thin gold/palladium layer (20 nm) before analysis.

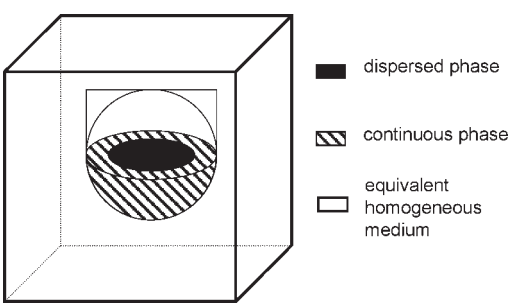

Figure 1 Illustration of a representative volume element (RVE) from the interlayer model.[18–19]

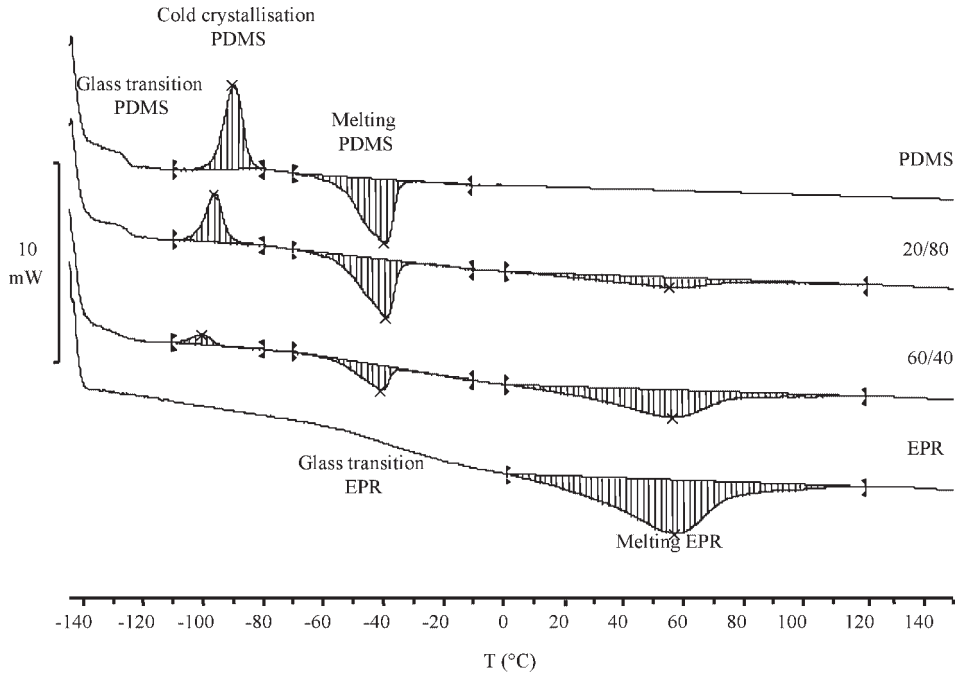

Figure 2 DSC scans of pure PDMS, pure EPR, and 60/40 and 20/80 EPR/PDMS (wt %) blends.

Theoretical considerations

The prediction of the dynamic mechanical properties of binary blends can be performed by self-consistent models.[18,19] Such a theoretical approach has been extensively described[18–21] previously and requires the definition of a representative volume element (RVE) consisting of concentric spheres embedded in an equivalent homogenous medium. The model used is the interlayer model,[18] which results in the following quadratic equation:

$$40|A|\left[\frac{E_b^*}{E_m^*}\right]^2 + (2|B| + 8|C|)\left[\frac{E_b^*}{E_m^*}\right] - 5|D| = 0$$

where E_b^* and $E_m^*$are the complex moduli in tension of the blend and the matrix, respectively; $|A|$, $|B|$, $|C|$, and $|D|$ are tenth order determinants with coefficients consisting of complex moduli, Poisson ratios, and volume fractions for the constituents, the matrix, interphase, and disperse phase. A detailed presentation of the coefficients of these determinants is available elsewhere.[21] The Poisson ratios (ν) used were: $\nu_{EPR} = 0.5$, $\nu_{PDMS} = 0.5$, and $\nu_{blend} = 0.5$.

The calculations in this paper are based on an RVE with two concentric spheres (i.e., without any interlayer). An illustration of one RVE is depicted in Figure 1. On the one hand, such a geometrical arrangement is representative of the morphology, the dispersed phase (phase 1) being covered by a shell of the continuous phase (phase 2). On the other hand, the blend composition is also taken into account in the calculations since the radii of the concentric spheres are chosen in accordance with the volume fractions of the different phases. Obviously, both PDMS and EPR can be con-

TABLE II
Experimental Characteristics from DSC and Density Measurements

SAMPLE		DSC measurements									
		Sample weight (mg)	PDMS phase					EPR phase		Density measurements	
Notation	PDMS wt %		T_g (°C)	Tα (°C)	T_m (°C)	ΔH_α (J/g)	ΔH_m (J/g)	T_m (°C)	ΔH_m (J/g)	Density (g/cm^3)	Lineary predicted density
EPR	0%	16.1	—	—	—	—	—	56 ± 1	43	0.89	0.89
U20	20%	14.1	—	—	—	—	—	55 ± 1	43	0.93	0.93
U40	40%	17.1	−129 ± 2	−100 ± 1	−41 ± 1	5	16	56 ± 1	42	0.98	0.98
U60	60%	13.1	−126 ± 2	−98 ± 1	−40 ± 1	5	18	56 ± 1	41	1.04	1.03
U80	80%	16.0	−125 ± 2	−97 ± 1	−40 ± 1	8	17	55 ± 1	44	1.11	1.11
PDMS	100%	14.6	−126 ± 2	−91 ± 1	−40 ± 1	13	17	—	—	1.16	1.16

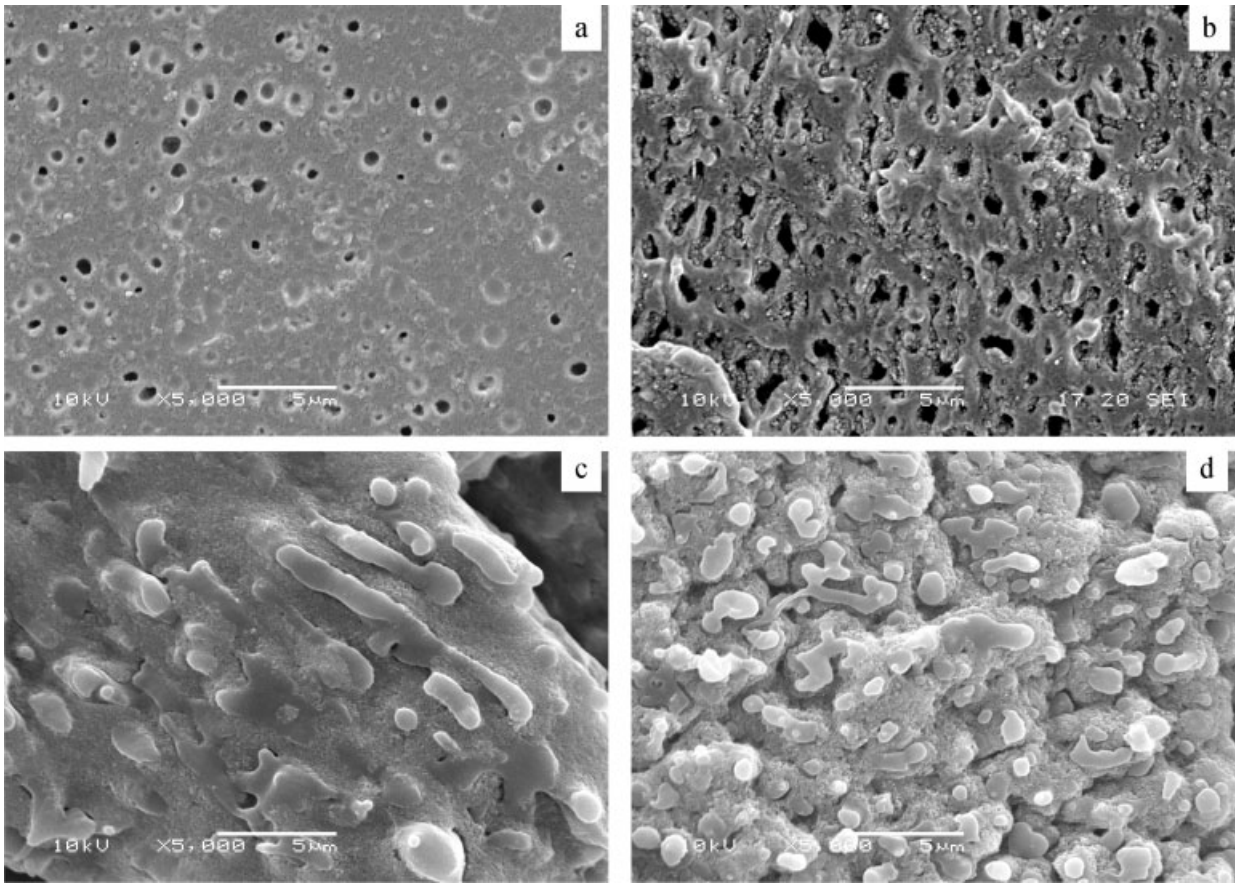

Figure 3 SEM micrographs of the EPR/PDMS (wt %) blends after 48 h etching: (a) 80/20, (b) 60/40, (c) 40/60, (d) 20/80.

sidered as dispersed phase in the numerical simulations, therefore leading to two theoretical predictions (depending on the geometrical arrangement in the RVE) for a unique blend composition.

RESULTS AND DISCUSSION

Density and DSC measurements

The DSC scans recorded for the pure constituents, and some representative blends (80/20 and 60/40) are given in Figure 2. When the temperature increases, several thermal transitions are evidenced. For the pure PDMS, there is a change in the heat capacity baseline at low temperature (around −126°C) that corresponds to its glass transition. This is then followed by an exothermic peak of cold crystallization (around −91°C) and by an endothermic melting peak (around −40°C). In the pure EPR the glass transition (around −40°C) as well as a broad melting peak (centered at 56°C) can be found. For the blends it can be noted that all the transitions of the pure constituents are present. However, the change in the heat capacity baseline corresponding to the EPR glass transition is overlapped by the PDMS melting peak and therefore remains undetected.

For all the samples, Table II summarizes the thermal characteristics corresponding to both EPR and PDMS phases, which are denoted as T_g (glass transition temperature, inflection point), T_{cc} (cold crystallization temperature), ΔH_{cc} (heat of fusion associated with the cold crystallization process), and ΔH_m (heat offusion associated with the melting process), respectively.

It can be noticed from Table II that ΔH_m of both EPR and PDMS phases in the blends remain constant and similar to that of the pure constituents. Therefore it can be concluded that the crystallization process of any of the components in the blends are not influenced by the presence of the other component.

Table II also reports on the density measurements obtained for the blends. In addition to the experimental values, a series of predicted values for the blend densities are given assuming a linear combination of the densities of the pure constituents in connection with the blend composition. No significant deviation of the blend densities compared to the predictions can be noticed.

Morphology

Figure 3 shows the SEM micrographs obtained for the four blends after etching in ethyl acetate for 48 h.

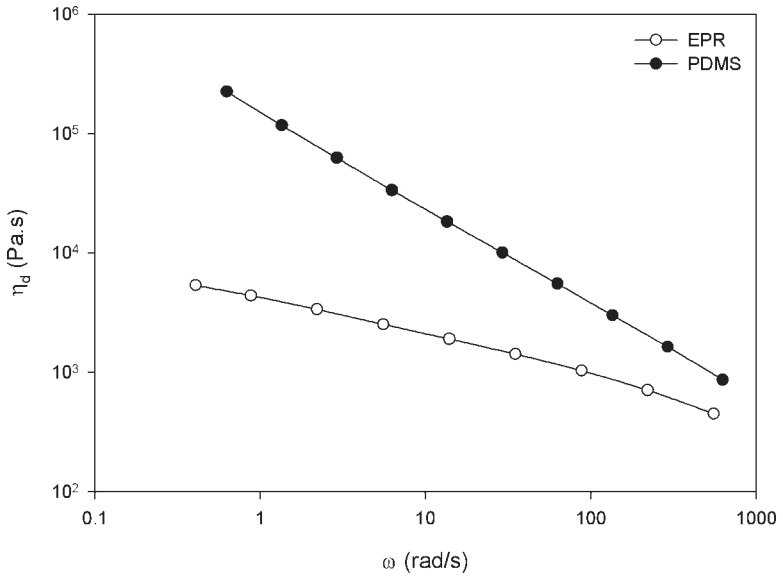

Figure 4 Dynamic viscosity of the pure constituents at 180°C.

Resulting from the removal of the PDMS phase that occurs during etching, the presence of holes is clearly observed in black on these micrographs. In addition a significant fine particular structure of remaining silica fillers is noticeable, in the range of 100 nm.

Figures 3(a) and (b) reveal a remaining matrix of EPR with dispersed small particles, in the size range of 1 μm, for the removed PDMS phase in the 80/20 and 60/40 samples. Figures 3(c) (40/60) and 3(d) (20/80) show a morphology that is hard to interpret, but from the images it seems likely that, even in these blends, which are based on a high PDMS content, the EPR phase forms the continuous phase.

To clarify the situation, dynamic viscosity measurements were performed. Figure 4 shows the dynamic viscosity of the pure constituents, η_d, as a function of the angular frequency, ω, at 180°C. It can be seen that the viscosity of the PDMS, while initially much higher than that of EPR, drops at a higher rate with the angular frequency compared to EPR. At higher frequencies both viscosities become close, and the viscosity ratio goes down toward 1.

The particle size of the dispersed phase, D, in melt mixed polymer blends is determined by the viscosity ratio, $\eta_{disperse}/\eta_{matrix}$, the effective shear rate, $\dot{\gamma}$ and the interfacial tension between the phases, σ_i, according to the following equation:[22]

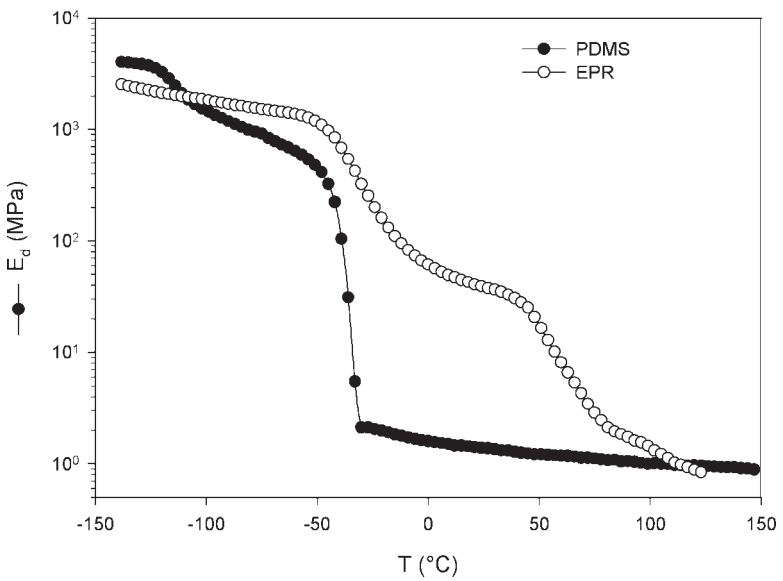

Figure 5 Viscoelastic properties at 1 Hz of the pure constituents: E_d versus temperature.

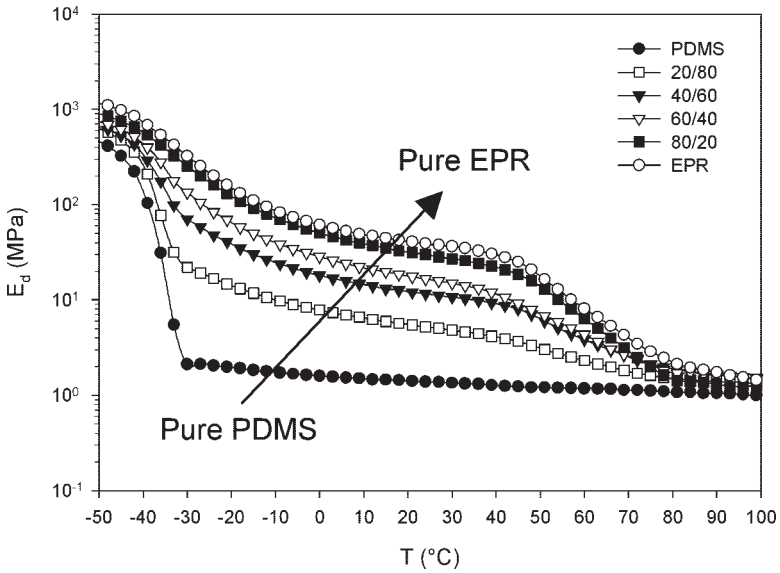

(a)

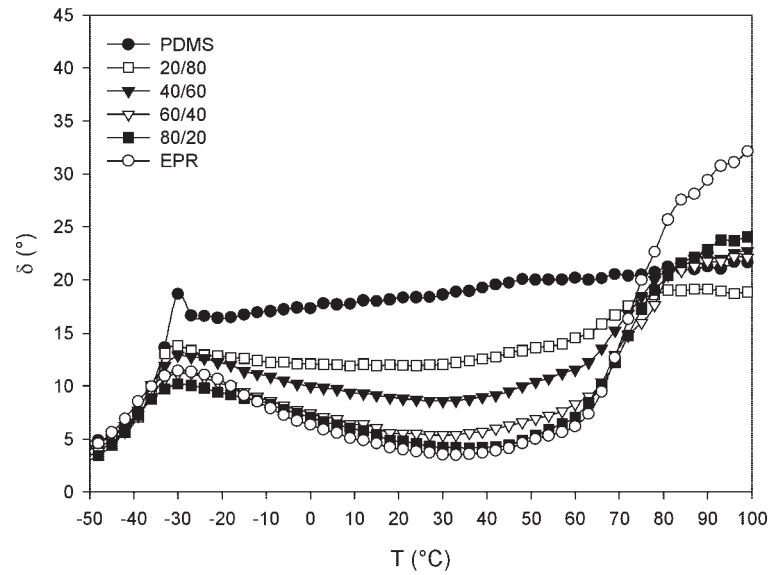

(b)

Figure 6 (a) Viscoelastic properties at 1 Hz of the EPR/PDMS blends: E_d versus temperature. The evolution of E_d of the pure constituents are recalled for comparison. (b) Viscoelastic properties at 1 Hz of the EPR/PDMS blends: δ versus temperature.

$$\frac{\dot{\gamma} \times \eta_{\text{matrix}} \times D}{\sigma_i} = 4 \times \left(\frac{\eta_{\text{disperse}}}{\eta_{\text{matrix}}}\right)^{0.84}$$

The interfacial tension between EPR and PDMS lies in the range of 3.9 mN/m, being a copolymer of PP and PE it should lie between $\sigma_{i,PP/PDMS} = 2.8$ and $\sigma_{i,PE/PDMS} = 5$ mN/m.[23] The shear rate is approximated as $\dot{\gamma} \sim n$, which is the screw speed in rpms,[22] thus $\dot{\gamma} = 100s^{-1}$ at present extruder conditions. The viscosites are available from Figure 4 with PDMS as the dispersed phase, $\eta_{\text{disperse}} = \eta_{\text{PDMS}} = 863$ Pa s and $\eta_{\text{matrix}} = \eta_{\text{EPR}} = 858$ Pa s. With these assumptions the equation predicts an average domain size in the order of 183 nm, which is lower than what was observed from the SEM images.

Viscoelastic properties

Figure 5 shows the temperature dependence of the dynamic modulus, $E_d (E_d = \sqrt{E'^2 + E''^2})$, for the pure constituents. From the drops in E_d values on the dynamic mechanical spectra, and with respect to the knowledge from the DSC curves, the transitions in the pure materials can be identified.

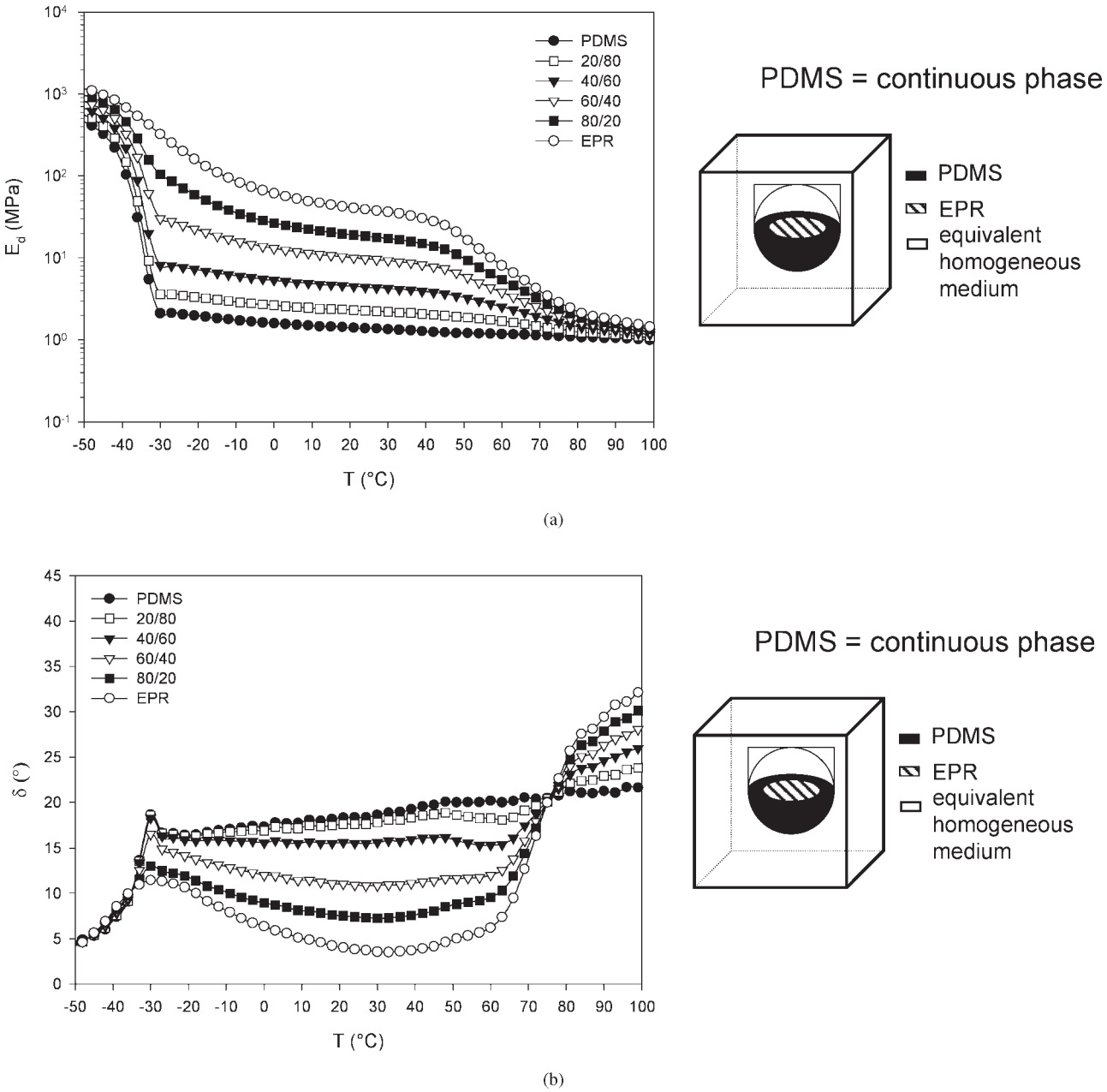

Figure 7 (a) Theoretical predictions at 1 Hz of viscoelastic properties considering PDMS as the continuous phase. (b) Theoretical predictions at 1 Hz of viscoelastic properties considering PDMS as the continuous phase.

For pure PDMS the main α-relaxation, associated with the glass transition, occurs around -110°C. Above -50°C the melting process of PDMS crystallites starts and leads to a dramatic drop in the mechanical properties. For the pure EPR the α-relaxation can be observed around -40°C, and the melting of the crystalline phase of the material occurs above 40°C.

The viscoelastic properties of the EPR/PDMS blends are given in Figures 6(a) and (b) for temperatures from -50 to 100°C. As the weight fraction of EPR becomes larger in the blends (see curves from 20/80 to 80/20), an increase of the values of the dynamic modulus can be noticed in the temperature range above -30°C. Therefore, it can be concluded that the presence of the EPR phase significantly improves the overall mechanical properties of the blends. Unfortunately, as already mentioned for the description of the DSC traces, both the melting of the crystallized PDMS phase and the α-relaxation of EPR overlap each other. As a consequence, the eventual changes in the molecular mobility of EPR (or PDMS) in the presence of PDMS (or EPR) cannot be discussed.

However, it was deemed to be of interest to associate DMA results and theoretical predictions of the viscoelastic properties of the blends.[24] In this way, numerical simulations were performed by using the

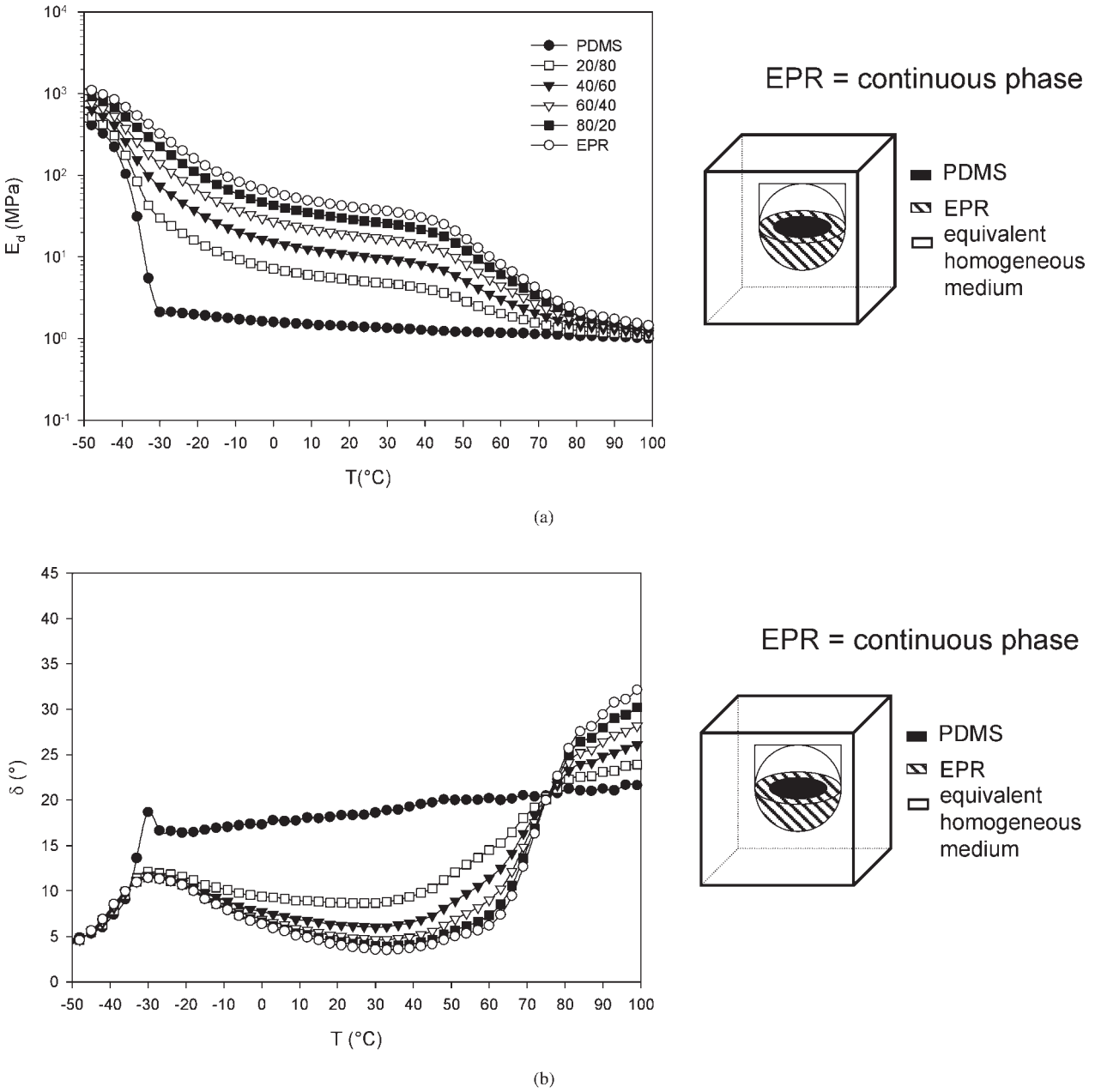

Figure 8 (a) Theoretical predictions at 1 Hz of viscoelastic properties considering EPR as the continuous phase. (b) Theoretical predictions at 1 Hz of viscoelastic properties considering EPR as the continuous phase.

interlayer model.[18] It is important to realize that, for a given blend composition, both EPR and PDMS can be considered either as the continuous or as the dispersed phase in the calculations. For such a purpose, the definition of two different RVEs (as depicted in Fig. 1) was required. Each of them is illustrated in Figures 7 and 8, where the theoretical predictions considering either PDMS (Fig. 7) or EPR (Fig. 8) as the continuous phase are given, for all the investigated blend compositions (the experimental evolutions of E_d for the pure PDMS and EPR are also recalled in these figures).

First of all, the comparison of both Figures 7 and 8 leads to the observation that, for a given blend composition, the theoretical evolutions of E_d are clearly distinct and are mainly influenced by the continuous phase. This is consistent with previous investigations[24] and is in agreement with Bohn's conclusions[25] indicating that the mechanical response of a polymer blend to a mechanical stress is very often dominated by that of the continuous phase.

As a consequence of such a distinction between the predictions considering one or the other phase as continuous, Figure 9 associates the experimental and the theoretical dynamic moduli E_d (at 25°C) [Fig. 9(a)], and phase angle δ [Fig. 9(b)], as a function of the PDMS weight content (i.e., the blend composition). It

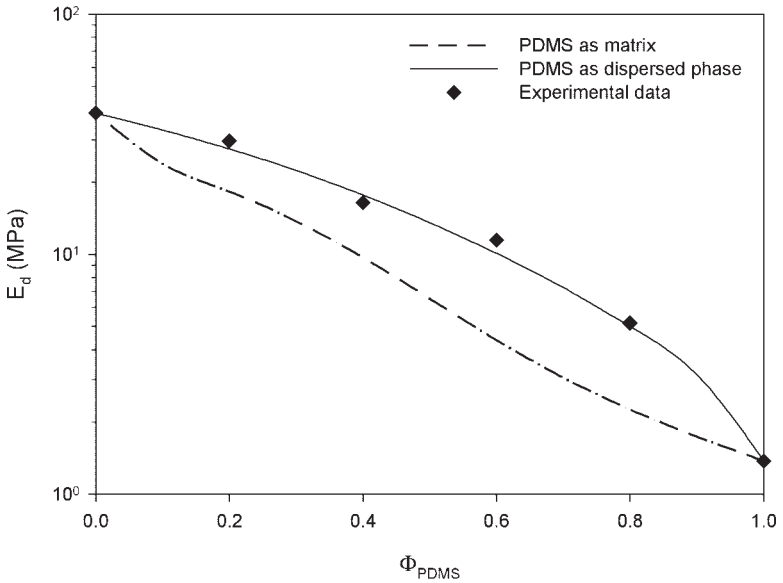

(a)

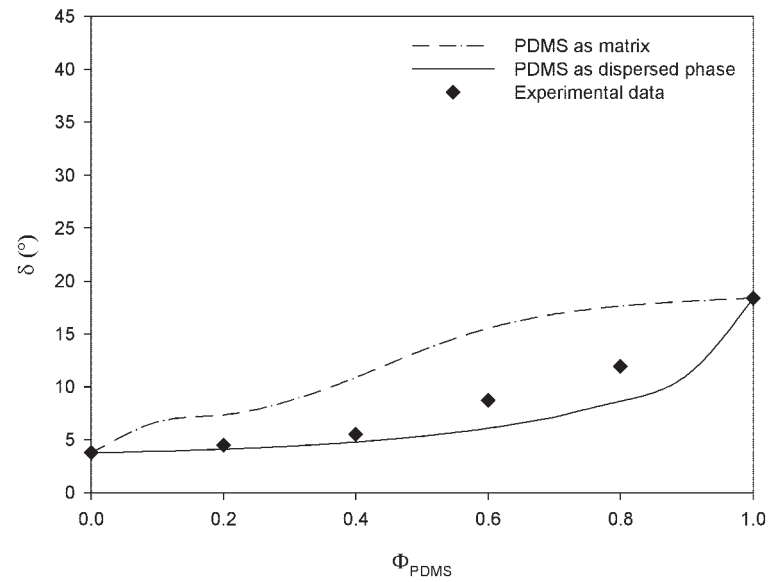

(b)

Figure 9 (a) Theoretical and experimental dynamic moduli, at 25°C and 1 Hz, as a function of the PDMS content. (b) Theoretical and experimental phase angles, at 25°C and 1 Hz, as a function of the PDMS content.

is clearly observed that the experimental data mainly follow the predicted curve considering EPR as the continuous phase and is thus in good agreement with our SEM observations. Such a combination (Fig. 9) of both experimental and theoretical viscoelastic data indicates that the EPR remains in the continuous phase in our binary EPR/PDMS melt mixed blends, independent of the blend composition.

CONCLUSION

We have studied and characterized a series of binary EPR/PDMS blends with regard to their mechanical viscoelastic properties in relation to their morphologies.

Density and DSC measurements showed that both density and crystallization processes are not affected by the blending process. SEM micrographs of etched samples revealed that the EPR remains continuous over the whole composition range. The fine dispersion of the PDMS phase in the EPR phase, which was observed in the SEM pictures, has been explained as resulting from the value of the viscosity ratio (estimated to be close to one during the meltmixing process).

The investigation of the viscoelastic properties of the samples showed a significant improvement of the

overall mechanical properties of the blends following the increase of the EPR content. In addition, the association of DMA results and mechanical modeling has been successfully used to confirm the blend morphology, in agreement with the SEM pictures.

The ELIS program of the foundation for strategic research (SSF) is gratefully acknowledged for their financial support. The authors also acknowledge Helen Hassander for assistance with the microscopy work and Henrik Eriksson for experimental assistance.

References

1. Hackam, R. IEEE Trans Dielectrics Electrical Insulation 1999, 6, 557.
2. Vlastos, A. E.; Gubanski, S. M. IEEE Trans Power Delivery 1991, 6, 888.
3. Owen, M. J.; Smith, P. J. J Adhes Sci Technol 1994, 8, 1063.
4. Chang, J. W.; Gorur, R. S. IEEE Trans Dielectrics Electrical Insulation 1994, 1, 1039.
5. Hillborg, H.; Gedde, U. W. IEEE Trans Dielectrics Electrical Insulation 1999, 6, 703.
6. Mitchell, J. M. Int Wire Cable Symp Proc 1986.
7. Kole, S.; Bhattacharya, A.; Tripathy, D. K.; Bhowmick, A. K. J Appl Polym Sci 1993, 48, 529.
8. Kole, S.; Chaki, T. K.; Bhowmick, A. K. Tripathy, D. K. Polym Degrad Stab 1993, 41, 109.
9. Kole, S.; Roy, S.; Bhowmick, A. K. Polymer 1994, 35, 3423.
10. Kole, S.; Roy, S.; Bhowmick, A. K. Polymer 1995, 36, 3273.
11. Kole, S.; Santra, R.; Bhowmick, A. K.Rubber Chem Technol 1994, 67, 119.
12. Kole, S.; Srivastava, S. K.; Tripathy, D. K.; Bhowmick, A. K. J Appl Polym Sci 1994, 54, 1329.
13. Geerts, Y.; Gillard, S.; Geuskens, G. Eur Polym J 1996, 32, 143.
14. Gornowicz, G. A.; Zhang. H. Dow Corning Corporation, USA, 2000.
15. Zhao, T. B.; Bernstorf, R. A. IEEE Electrical Insulation Mag 1998, 14, 26.
16. Saleem, M.; Baker, W. E. J Appl Polym Sci 1990, 39, 655.
17. Utracki, L. A. Polymer Alloys and Blends; Hanser Publishers, Munich, 1990.
18. Maurer, F. H. J. In Polymer Composites; Sedlacek, B., Ed.; W. de Gruyter & Co.: Berlin, 1986; p. 399.
19. Maurer, F. H. J. In Controlled Interphases in Composite Materials; Ishida, H., Ed.; Elsevier Science: New York, 1990; p. 491.
20. Eklind, H.; Maurer, F. H. J. Polymer 1996, 37, 2641.
21. Colombini, D.; Maurer, F. H. J. Macromolecules 2002, 35, 5891.
22. Wu, S. H. Polym Eng Sci 1987, 27, 335.
23. Wu, S. H. Polymer Interface and Adhesion; Marcel Dekker: New York, 1982.
24. Colombini, D.; Merle, G.; Alberola, N. D. J Appl Polym Sci 2000, 76, 530.
25. Bohn, L. In Copolymers, Polyblends and Composites: A Symposium; Platzer, N. A. J., Ed.; Washington, Adv Chem Ser, Am Chem Soc, 1974; p 66.